

A New Feature Selection Method for LogNet and its Application for Diagnosis and Prognosis of COVID-19 Disease Using Routine Blood Values

Mehmet Tahir Huyut ^{1,*} and Andrei Velichko ²

¹ Department of Biostatistics and Medical Informatics, Faculty of Medicine, Erzincan Binali Yildirim University, Erzincan, Turkey

² Institute of Physics and Technology, Petrozavodsk State University, 33 Lenin str., 185910, Petrozavodsk, Russia

* Correspondence: tahir.huyut@erzincan.edu.tr (M.T.H); velichko@petsu.ru (A.V.)

Abstract: Since February-2020, the world has embarked on an intense struggle with the COVID-19 disease, and health systems have come under a tragic pressure as the disease turned into a pandemic. The aim of this study is to determine the most effective routine-blood-values (RBV) in the diagnosis/prognosis of COVID-19 using new feature selection method for LogNet reservoir neural network. First dataset in this study consists of a total of 5296-patients with a same number of negative and positive covid test. Second dataset consists of a total of 3899-patients with a diagnosis of COVID-19, who were treated in hospital with severe-infected (203-patients) and mildly-infected (3696-patients). The most important RBVs that affect the diagnosis of the disease from the first dataset were mean-corpuscular-hemoglobin-concentration (MCHC), mean-corpuscular-hemoglobin (MCH) and activated-partial-prothrombin-time (aPTT). The most effective features in the prognosis of the disease were erythrocyte-sedimentation-rate (ESR), neutrophil-count (NEU), C-reactive-protein (CRP). LogNet-model achieved an accuracy rate of $A_{46} = 99.5\%$ in the diagnosis of the disease with 46 features and $A_3 = 99.17\%$ with only MCHC, MCH, and aPTT features. Model reached an accuracy rate of $A_{48} = 94.4\%$ in determining the prognosis of the disease with 48 features and $A_3 = 82.7\%$ with only ESR, NEU, and CRP features. LogNet model demonstrated a very high disease diagnosis/prognosis of COVID-19 performance without knowing about the symptoms or history of the patients. The model is suitable for devices with low resources (3-14 kB of RAM used on the Arduino microcontroller), and is promising to create mobile health monitoring systems in the Internet of Things. Our method will reduce the negative pressures on the health sector and help doctors understand pathogenesis of COVID-19 through key features and contribute positively to the treatment processes.

Keywords: COVID-19; biochemical and hematological biomarkers; routine blood values; feature selection method; LogNet neural network; Internet of Medical Things; IoT.

1. Introduction

The new severe acute respiratory syndrome coronavirus (SARS-CoV-2), first identified in 2019, has rapidly affected the world and caused a pandemic [1,2]. The disease, identified as coronavirus 2019 (COVID-19), can cause severe pneumonia and fatal acute respiratory distress syndrome (ARDS) [3–6]. While the disease may be asymptomatic, severe ARDS is thought to be due to the inflammatory cytokine storm that may be encountered during this period [6,7]. As a matter of fact, it has been stated in previous studies

that this pathogen can cause a serious respiratory disorder that requires special intervention in intensive care units (ICUs) and in some cases may cause death [6,7]. Moreover, the symptoms of COVID-19 induced by the new SARS-CoV-2 are difficult to distinguish from known infections in the majority of patients [6,8,9].

Previous studies have demonstrated the clinical importance of changes in the routine blood parameters (RBV) in the diagnosis and prediction of prognosis of infectious diseases [1–4,10,11]. Similarly, many abnormalities have been reported in the peripheral blood of patients infected with COVID-19 [6,7,11]. However, Jiang et al. [12] and Zheng et al. [13] emphasized that information on early predictive factors for particularly severe and fatal COVID-19 cases is relatively limited and further research is needed. Huyut et al. [6] and Lippi et al. [14] described that the rapid spread of disease in pandemics overwhelms health systems and raises concerns about the need for intensive care treatment. Rapid spread of the disease in pandemics overwhelms the health system, raising concerns about the need for intensive care treatment [6,14]. In addition, it has been reported that the detection of severe and mild patients in COVID-19 is an important and clinically difficult process in terms of morbidity and mortality [6]. Despite these clinical features of COVID-19, studies with large samples representing laboratory abnormalities of patients are needed [3,15]. Therefore, the relationship between Covid-19 disease and RBVs should be supported by large datasets.

For this reason, it has been the focus of studies to determine whether patients who are likely to benefit from supportive care and early intervention are at risk and how to identify them [6,11]. While new tests are being developed for the diagnosis of COVID-19, Banerjee et al. [8] stated that these applications require specialized equipment and facilities. Accordingly, estimating the diagnosis/prognosis of diseases without using advanced devices and methods; It can help with various problems such as patient comfort, health systems and economic inefficiencies. For this purpose, Beck et al. [16] and Xu et al. [17] reported that more economical and faster alternative methods are being developed to assist clinical procedures.

Uncertainties in the routine blood values of COVID-19 patients, difficulties in diagnosis and treatment have increased the interest in machine learning (ML) and artificial intelligence (AI) approaches from the alternative methods. The most important reason for this is the power of artificial intelligence models to reveal hidden relationship structures between features [18]. In this context, artificial intelligence approaches are frequently used in real-time decision making to reduce drug costs, improve patient comfort and improve the quality of healthcare services [5,18].

There are several attempts in existence that use artificial intelligence methods to predict the diagnosis and mortality of COVID-19 [4,16]. Most of these studies relied on computed tomographic (CT) [19], while far fewer relied on RBVs [4,5,19]. However, imaging-based solutions are costly, time-consuming and require specialized equipment [19]. In this context, some studies [5,19,20] have highlighted that diagnosis based on RBV values can provide an effective, rapid and cost-effective alternative for early detection and prognosis of COVID-19 cases.

However, previous AI studies did not use most of the RBV parameters and reported relatively poorer classifier performance to this study [2,3,5,6]. Also, previous studies [8,18–24], have generally focused on the early diagnosis of COVID-19 disease and have addressed relatively smaller samples. In addition, artificial intelligence studies on predicting the prognosis of the disease and detecting severely or mildly infected patients in the early period based on RBVs alone are insufficient. It was stated that studies to be carried out for this purpose could reduce the intensity on the ICU and help health services by detecting severe and mildly infected patients with COVID-19 early [2,5,18,19].

The most ML are the process of transforming the feature vector from the first multidimensional space to the second multidimensional space and detecting it by a linear classifier [25]. The differences between ML models generally lie in the transformation algorithms and their number and order. In addition, transformation algorithms can be in the

form of reducing and increasing the space dimension. The popular machine learning classifier algorithms commonly used for data analysis are: multilayer perceptron (feedforward neural network with several layers, linear classifier) [26], support vector machine [27], K-nearest neighbors method [28], XGBoost classifier [29], random forest method [30], logistic regression [31], decision trees [32].

ML algorithms typically require a sufficiently large number of samples. However, in this case, the dataset has to be reduced for reasons related to the dimensionality problem. This is achieved by finding a matrix that has fewer columns and is similar to the original. Since this matrix consists of fewer features, it can be used more efficiently than the original matrix. Dimensionality reduction can be defined as the process of finding matrices with fewer columns. The feature selection is one of the techniques used to reduce dimensionality; In this technique, irrelevant and redundant features are discarded while selecting the relevant features [25,33]. Also, the selection of appropriate features can reduce the measurement cost and provide a better understanding of the problem [25]. Feature selection methods can be classified as filters, embedded methods, and wrappers, depending on their relationship to the learning method [25,33]. Because feature selection is part of the training process in embedded methods, this method lies between filters and wrappers. Searching for the best subset of features is performed during training of the classifier (for example, when optimizing weights in a neural network) and therefore embedded methods have less computational cost than wrappers [25].

Most of the new feature selection methods are filters, although we can find representative methods for all three categories [25]. The large numbers of feature selection methods currently available complicate the selection of the best method for a given problem [33]. Below are the latest methods that have become popular among researchers: Feature Selection Based on Correlation (CFS) [34], Filtering Based on Consistency [35], INTERACT [36], Knowledge Gain (InfoGain) [37], ReliefF [38], Recursive Feature Elimination for Support Vector Machines (SVM-RFE) [39], Lasso editing [40], Minimum Redundancy Maximum Relevance (mRMR) algorithm (developed specifically for dealing with microarray data) [25].

In our previous published study [41], a classifier based on LogNNet neural network was described using handwriting recognition example from MNIST database. Velichko [42] demonstrated the use of the LogNNet to calculate risk factors for the presence of a disease based on a set of medical health indicators. The LogNNet neural network is a direct distribution network that improves classification accuracy by passing the feature vector through a special reservoir matrix and transforming it into a feature vector of different size [43]. Previous studies have shown that the higher the entropy of a chaotic mapping that fills a reservoir matrix, the better the classification accuracy [44]. Therefore, the procedure for optimizing chaotic map parameters plays an important role in the presented data analysis method using LogNNet neural network. In addition, due to the characteristics of chaotic mapping, it is possible to significantly reduce RAM memory usage by a neural network. For this purpose, in a study [42], the algorithm of LogNNet operation on a device with 2 kB of RAM was presented. This result showed that LogNNet can be used in Internet of Things (IoT) mobile devices.

In this study, 3 main stages can be distinguished: data collection, LogNNet training with selection of main features and testing of feature combinations (Figure 1). Between the specified dates, the RBV results of the patients measured at admission were recorded retrospectively. Two different data sets were created from the obtained data. The first dataset includes the information of 2648 outpatients diagnosed with COVID-19 and the same number of patients who tested negative for COVID-19. The second dataset contains the information of 3899 patients (ICU and non-ICU) who were hospitalized with the diagnosis of COVID-19. The most effective RBV values (features) in the diagnosis and prognosis of COVID-19 were determined by a new feature selection method. Next, the performance of the LogNNet neural network model fed by main features and combinations of selected features in predicting the diagnosis/prognosis of the disease was evaluated.

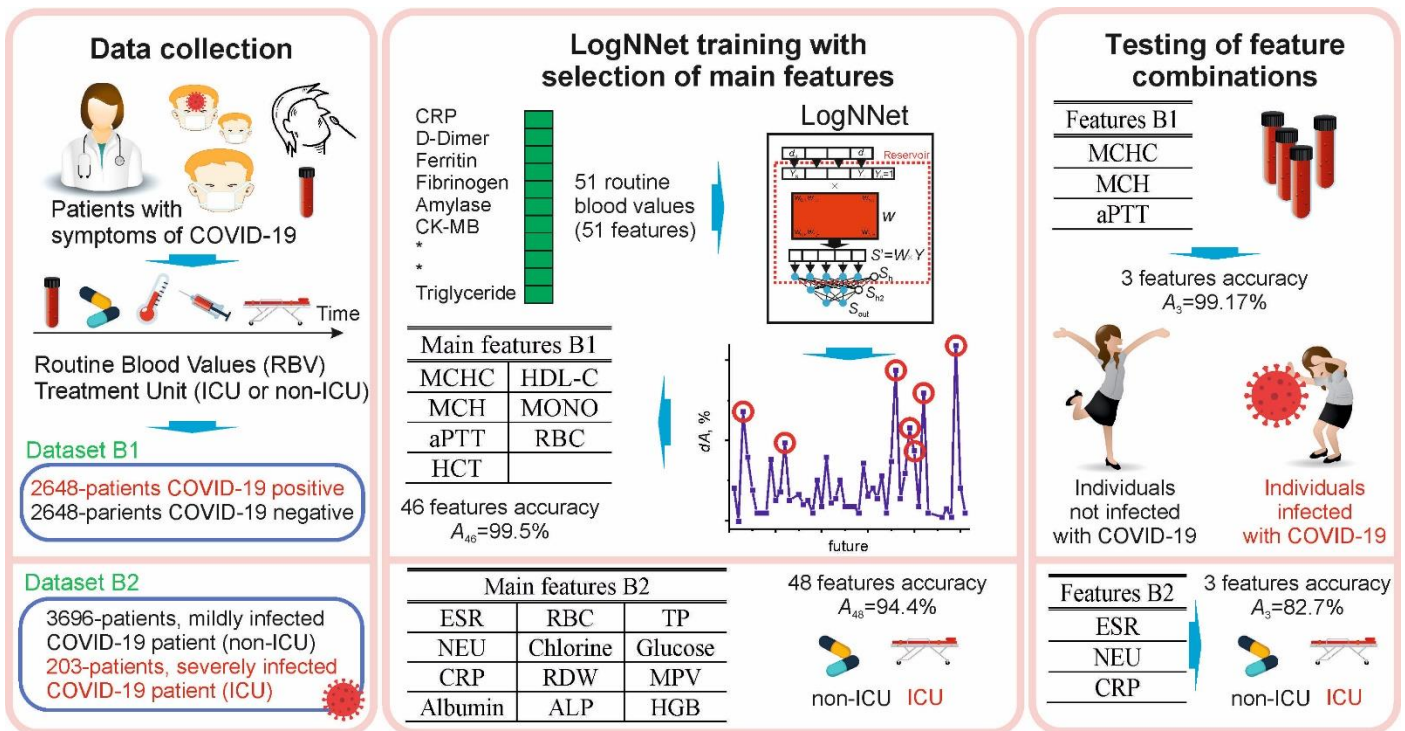


Figure 1. The main stages of the study for the diagnosis/prognosis of COVID-19 using the routine blood values: data collection, LogNNet training with the selection of main features, testing combinations of the most important features that influence the diagnosis/prognosis of the disease.

The paper has the following structure. Section 2 describes data collection procedure, the basic LogNNet architecture, K-fold cross-validation technique, followed by sections describing the new feature selection method for LogNNet. Section 3 describes two examples of using the feature selection methodology for two datasets. In this section, the most important RBVs (features) effective in the diagnosis and prognosis of the disease were selected. Using various combinations of these features, the performance of the LogNNet model in the diagnosis and prognosis of the disease was calculated. Section 4 discusses the results and compares them with known developments. In Conclusion, a general description of the study and its scientific significance are given.

2. Materials and Methods

This study was conducted in accordance with the 1989 Declaration of Helsinki. Data matching to our criteria were collected retrospectively from the information system of Erzincan Binali Yıldırım University Mengücek Gazi Training and Research (EBYU-MG hospital) Hospital between April-December 2021 and included in the study.

The RBV of the patients consisted of biochemical, hematological and immunological tests. Severely infected patients were defined as the intensive care unit (ICU), while mildly infected patients were defined as non-ICU (subjects in all wards). Dataset B1 included information on $n = 2648$ outpatient COVID-19 positive and $n = 2648$ COVID-19 negative (control group) total 5296 patients. In the B2 dataset, there were information of $n = 203$ ICU and $n = 3696$ non-ICU COVID-19 patients. Raw data recorded included patients' diagnoses (COVID-19, heart disease, asthma, etc.), treatment units (ICU or non-ICU), age, and RBV data. The entire recording process took 20 hours. In the raw data, RBV data were on a quantitative scale, diagnostic data were on a multinomial scale, and treatment units were on a binomial scale. In the data preprocessing stage, the string data was converted into numerical data. Categorical data were coded, repeated measurements were averaged, duplicates were removed, and quantitative data were normalized. The missing RBV data were complemented by the mean of the respective parameter distribution

2.1. Characteristic of Participants, Workflow and Define Datasets

In the EBYU-MG hospital, only the cases that were detected as SARS-CoV-2 by real-time reverse transcriptase polymerase chain reaction (RT-PCR) in nasopharyngeal or oropharyngeal swabs during the dates covered by this study were diagnosed with COVID-19. The research only included individuals over the age of 18. In order to prevent various complications, RBV results at the first admission were recorded.

First data set (B1) includes the information of 2648 patients diagnosed with COVID-19 and receiving outpatient treatment in hospital on the specified dates, and the same number of patients (control group) whose COVID-19 tests were negative. With our new feature selection procedure, the most important RBV features that are effective in the diagnosis of the disease were selected from the B1 dataset. The selected features were fed into LogNet neural network to examine the method's performance in diagnosing COVID-19 disease.

Second data set (B2) includes the information of 3899 patients who were treated for COVID-19 in hospital on the specified dates. The treatment units of these patients at the first admission were examined. In the B2 dataset, there were $n = 203$ ICU and $n = 3696$ non-ICU COVID-19 patients. Then, with our new feature selection procedure, the most influential RBV traits in the prognosis of the disease were selected from the B2 dataset. Selected features were fed into the LogNet deep neural network to examine the performance of this method in determining the prognosis/severity of COVID-19 disease.

The B1 and B2 data sets used in this study are presented in Table 1 and Table 2. B1 and B2 datasets include immunological, hematological and biochemical RBV parameters and each dataset consists of 51 features. In the B1 data set, positive COVID-19 test results were coded as 1 and negative as 0 (COVID-19 = 1, non-COVID-19 = 0).

In the B2 dataset, severely infected (ICU) COVID-19 patients were coded as 1, while mildly infected (non-ICU) COVID-19 patients were coded as 0 "ie: ICU COVID-19 = 1", "non-COVID-19 = 0". Datasets can be downloaded in Supplementary Materials of this paper.

Table 1. Feature numbering for B1 datasets.

N ^o	Feature	N ^o	Feature	N ^o	Feature	N ^o	Feature	N ^o	Feature
1	CRP	12	NEU	23	MPV	34	GGT	45	Sodium
2	D-Dimer	13	PLT	24	PDW	35	Glucose	46	T-Bil
3	Ferritin	14	WBC	25	RBC	36	HDL-C	47	TP
4	Fibrinogen	15	BASO	26	RDW	37	Calcium	48	Triglyceride
5	INR	16	EOS	27	ALT	38	Chlorine	49	eGFR
6	PT	17	HCT	28	AST	39	Cholesterol	50	Urea
7	PCT	18	HGB	29	Albumin	40	Creatinine	51	UA
8	ESR	19	MCH	30	ALP	41	CK		
9	Troponin	20	MCHC	31	Amylase	42	LDH		
10	aPTT	21	MCV	32	CK-MB	43	LDL		
11	LYM	22	MONO	33	D-Bil	44	Potassium		

CRP: C-reactive protein; INR: international normalized ratio; PT: prothrombin time; PCT: Procalcitonin; ESR: erythrocyte sedimentation rate; aPTT: activated partial prothrombin time; LYM: lymphocyte count; NEU: neutrophil count; PLT: platelet count; WBC: white blood cell count; BASO: basophil count; EOS: eosinophil count; HCT: hematocrit; HGB: hemoglobin; MCH: mean corpuscular hemoglobin; MCHC: mean corpuscular hemoglobin concentration; MCV: mean corpuscular volume; MONO: monocyte count; MPV: mean platelet volume; PDW: platelet distribution width; RBC: red blood cells; RDW: red cell distribution width; ALT: alanine aminotransaminase; AST: aspartate aminotransferase; ALP: alkaline phosphatase; CK-MB: creatine kinase myocardial band; D-Bil: direct bilirubin; GGT: gamma-glutamyl transferase; HDL-C: high-density lipoprotein-cholesterol; CK: creatine kinase; LDH: lactate dehydrogenase; LDL: low-density lipoprotein; T-Bil: total bilirubin; TP: total protein; eGFR: estimating glomerular filtration rate; UA: uric acid.

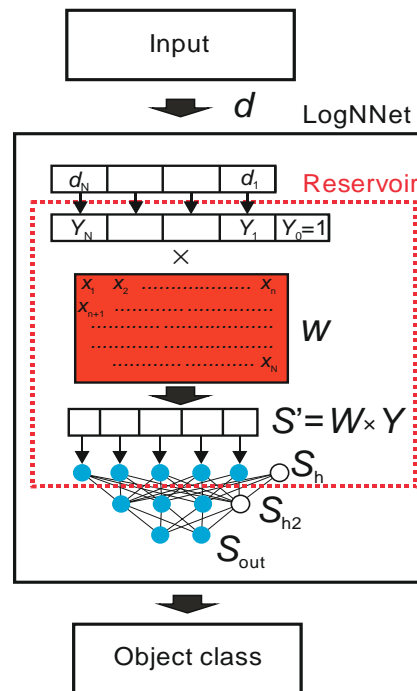
Table 2. Feature numbering for B2 datasets.

Nº	Feature	Nº	Feature	Nº	Feature	Nº	Feature	Nº	Feature
1	ALT	12	Chlorine	23	eGFR	34	MONO	45	Fibrinogen
2	AST	13	Cholesterol	24	Urea	35	MPV	46	INR
3	Albumin	14	Creatinine	25	UA	36	NEU	47	PT
4	ALP	15	CK	26	BASO	37	PDW	48	PCT
5	Amylase	16	LDH	27	EOS	38	PLT	49	ESR
6	CK-MB	17	LDL	28	HCT	39	RBC	50	Troponin
7	D-Bil	18	Potassium	29	HGB	40	RDW	51	aPTT
8	GGT	19	Sodium	30	LYM	41	WBC		
9	Glucose	20	T-Bil	31	MCH	42	CRP		
10	HDL-C	21	TP	32	MCHC	43	D-Dimer		
11	Calcium	22	Triglyceride	33	MCV	44	Ferritin		

ALT: alanine aminotransaminase; AST: aspartate aminotransferase; ALP: alkaline phosphatase; CK-MB: creatine kinase myocardial band; D-Bil: direct bilirubin; GGT: gamma-glutamyl transferase; HDL-C: high-density lipoprotein-cholesterol; CK: creatine kinase; LDH: lactate dehydrogenase; LDL: low-density lipoprotein; T-Bil: total bilirubin; TP: total protein; eGFR: estimating glomerular filtration rate; UA: uric acid; BASO: basophil count; EOS: eosinophil count; HCT: hematocrit; HGB: hemoglobin; LYM: lymphocyte count; MCH: mean corpuscular hemoglobin; MCHC: mean corpuscular hemoglobin concentration; MCV: mean corpuscular volume; MONO: monocyte count; MPV: mean platelet volume; NEU: neutrophil count; PDW: platelet distribution width; PLT: platelet count; RBC: red blood cells; RDW: red cell distribution width; WBC: white blood cell count; CRP: C-reactive protein; INR: international normalized ratio; PT: prothrombin time; PCT: procalcitonin; ESR: erythrocyte sedimentation rate; aPTT: activated partial prothrombin time.

2.2. LogNet architecture

Figure 2 shows a principle of operation of the neural network LogNet [42].

**Figure 2.** LogNet architecture [42].

An object in the form of a feature vector, denoted as d , is input to LogNet. The feature vector contains N coordinates (d_1, d_2, \dots, d_N), where the number N is defined by the user. The classifier output determines the object class to which the input feature vector d

belongs. The number of possible classes denoted as M . LogNNet contains a reservoir with a special matrix, denoted as W . The matrix W was filled row by row with numbers generated by the chaotic mapping x_n . In this paper, it is proposed to use chaotic mapping based on congruential generator formula (1) (see Table 3), and Algorithm of matrix W filling shown in Table 4. Vector d converted into a vector Y of dimension $N+1$ with an additional coordinate $Y_0 = 1$ and each component is normalized by dividing by the maximum value of this component in the training base. Then there is a multiplication of a special matrix W , dimension $(N+1) \times P$ and a vector Y . The result is a vector S' with P coordinates, which is normalized [41] and converted into a vector S_h of dimension $P+1$ with zero coordinate $S_h[0] = 1$, which plays the role of a bias element. Thus, the primary transformation of the feature vector d into the second $(P+1)$ -dimensional space takes place. Then the vector S_h is fed to a two-layer linear classifier, with the number of neurons H in the hidden layer S_{h2} , and the number of outputs M in the output layer S_{out} . To indicate the parameters of the neural network, the short designation LogNNet $N:P:H:M$ is used.

The training of the linear classifier LogNNet was carried out using the backpropagation method [41].

Table 3. Chaotic map formula and list of optimized parameters with limits.

Chaotic map	List of optimized parameters (limits)	Formula
Congruent generator	K (-100 to 100) D (-100 to 100) L (2 to 10000) C (-100 to 100)	$\begin{cases} x_{n+1} = (D - K \cdot x_n) \bmod L \\ x_1 = C \end{cases} \quad (1)$

Table 4. Algorithm of matrix W filling.

```

xn: = C;
for j: = 1 to P do
for i: = 0 to N do
begin
xn: = (D-K*xn) mod L; // Congruential generator formula
W[i,j]: = xn/L;
end;

```

2.3. Optimization of reservoir parameters

The optimal chaotic mapping parameters were selected using a special algorithm and their range is indicated in Table 3. Before optimization, it is necessary to set the values of the constant parameters of the model: the value $P+1$, which determines the dimension of the vectors S_h and S_{h2} , the number of layers in the linear classifier, the number of epochs Ep for backpropagation training, the number of neurons in the classifier's hidden layer, in the case of a two-layer classifier. Then the training of the LogNNet network begins, performed by two nested iterations [45]. The inner iteration trains the output LogNNet classifier by backpropagation the error on the training set, the outer iteration optimizes the model parameters.

During the optimization process, the training and validation bases coincided and were equivalent to the initial datasets (B1 or B2). The outer iteration is implemented on the basis of the particle swarm method with fitness function equal to classification accuracy. Exit from outer iteration occurs either when the desired values of the classification accuracy are reached, or when the specified number of iterations in the particle swarm method is reached. As a result, we obtain optimized model parameters (chaotic mapping parameters) at the output, which allow us to obtain the highest classification accuracy on the validation set.

2.4. K-fold cross-validation technique

K-fold cross-validation technique was used to test LogNNNet, it is very well suited for medical databases where there is no splitting into test and training sets. The elements of the set (B1 or B2) are divided into K parts ($K = 5$), and then one of the parts is taken as the test sample, and the remaining $K-1$ parts are for the training sample. Then the average value of the metrics is calculated for all K cases when one of the K parts of the set becomes the test sample in turn. A distinctive feature of the method is that the test data should not be involved in the training process. Results the application of K-fold cross-validation technique allowed to calculate the classification metrics: A -classification accuracy, Precision, Recall and F1-metric. According to the text of the article, wherever we talk about the classification accuracy A , the value obtained by the K-fold cross-validation method is implied.

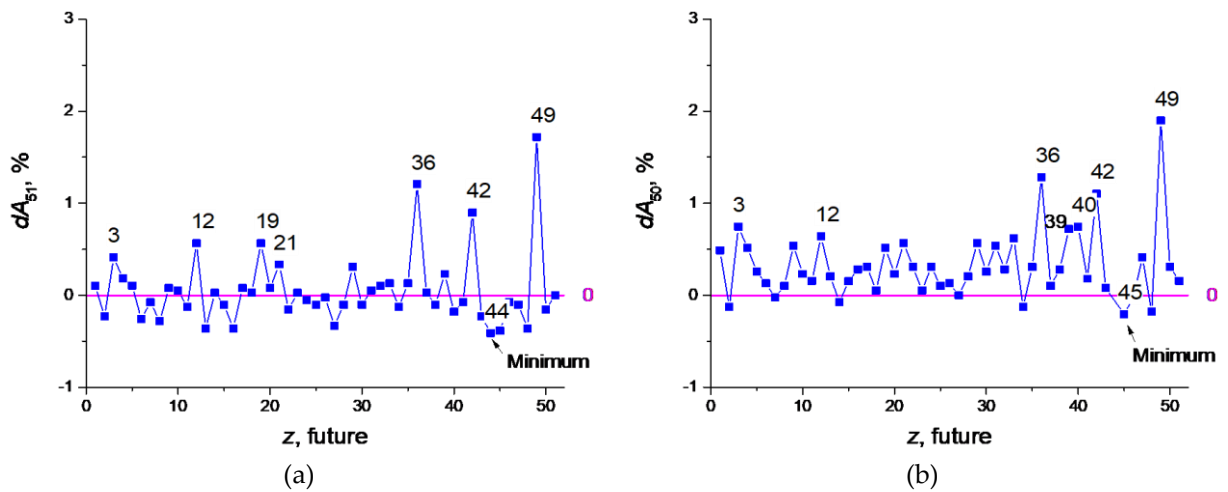
To obtain a higher value of A , the training $K-1$ parts of the sets were balanced according to the method from [42]. It includes the alternation of vectors from all classes with equalization of their numbers by the duplication method.

2.5. Future selection method

The feature selection method is based on two consecutive steps. First, we need to remove features that make it difficult to train the neural network and are redundant. The second stage involves sorting the remaining features according to their contribution to the classification metric. The features are removed by zeroing the corresponding components of the input vectors d .

The implementation of this approach is shown on the example of futures selection for the base B2. Suppose a reservoir optimization was carried out and an accuracy of $A_{51} = 93.665\%$ was obtained (using K-fold cross-validation), here the designation A_{NF} is introduced - classification accuracy when using $NF = 51$ features. Let us introduce additional pointers, denote the set of removed features by FR , and denote the set of selected features by FS . For example, $A_{49}(FR[3, 33])$ denotes accuracy at $NF = 49$ features with features $z = 3$ and $z = 33$ removed, and $A_4(FS[1, 22, 33, 41, 55])$ denotes accuracy at $NF = 4$ features with the main features from the set FS , $z = 1, 22, 33, 41, 55$. Next, we plot the dependence of the value of dA_{51} on the number of the removed feature z (see Figure 3a), where

$$dA_{51}(z) = A_{51} - A_{50}(FR[z]) \quad (2)$$



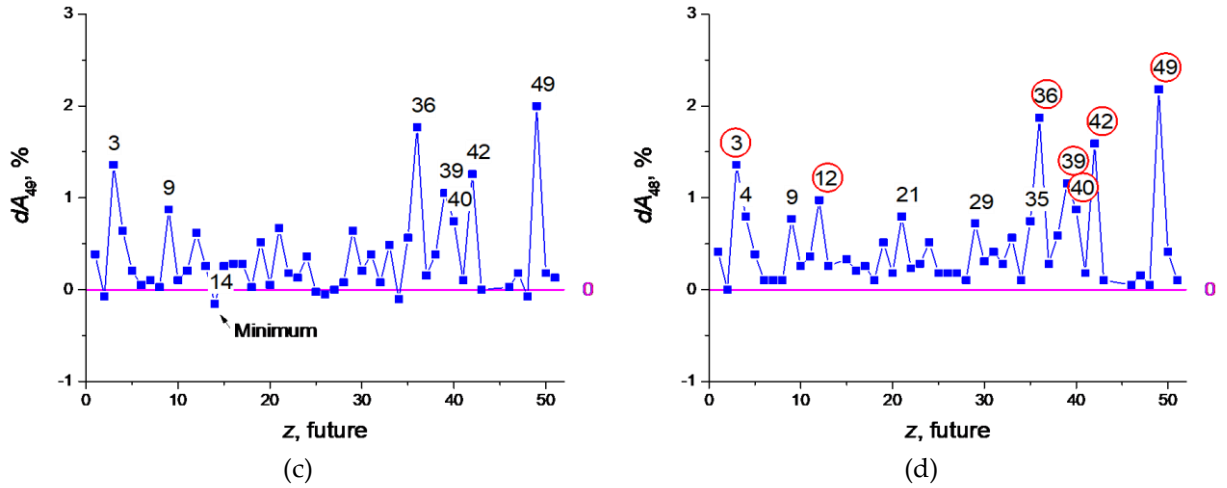


Figure 3. Function of the feature strength $dA_{51}(z)$ (a), $dA_{50}(z)$ (b), $dA_{49}(z)$ (c), $dA_{48}(z)$ (d).

Dependence $dA(z)$ will be defined as a function of the feature strength. The value $A_{50}(FR[z])$ characterizes the classification accuracy of the neural network using $NF = 50$ features, after deleting the feature with number z . Positive feature strength dA_{51} (Figure 3a and Equation 2) means that the removal of the feature reduces the classification accuracy of the network and the feature is useful, and negative dA_{51} means that the feature interferes with learning (redundant) and its removal leads to an increase in the classification properties of the neural network. According to Figure 3a, seven most useful features can be identified after the first selection iteration with numbers $z = 49, 36, 42, 19, 12, 3, 21$. The feature that makes learning the most difficult is number $z = 44$ (in Figure 3 it is indicated by the index 'Minimum') at its removal $A_{50}(FR[44]) = 94.075\%$, which exceeds the previous value $A_{51} = 93.665\%$.

The next iteration involves calculating the dependence of $dA_{50}(z)$, where

$$dA_{50}(z) = A_{50}(FR[44]) - A_{49}(FR[44, z]) \quad (3)$$

Its graph has the form shown in Figure 3b. Equation (3) implies the exclusion of the worst feature $z = 44$ and the exclusion of all other features in turn. As a result, the next feature to exclude will be feature $z = 45$, and the best accuracy will be $A_{49}(FR[44, 45]) = 94.28\%$.

Iterations continue until all dA values are greater than or equal to zero. Figures 3c,d show graphs for equations (4, 5)

$$dA_{49}(z) = A_{49}(FR[44, 45]) - A_{48}(FR[44, 45, z]) \quad (4)$$

$$dA_{48}(z) = A_{48}(FR[44, 45, 14]) - A_{47}(FR[44, 45, 14, z]) \quad (5)$$

The graph in Figure 3d contains the dependence $dA_{48}(z)$ which lies above the zero value. Thus, the best classification accuracy corresponds to $A_{48}(FR[44, 45, 14]) = 94.434\%$, after removing the features $z = 44, 45, 14$. During the selection, the set of the best seven features with highest future strength dA also changed from the set $[49, 36, 42, 19, 12, 3, 21]$ (Figure 3a) to $[49, 36, 42, 3, 39, 12, 40]$ (Figure 3d, red circle).

The second stage consists in arranging features according to their effectiveness (strength) in descending order of peak values dA . For the considered example, such a sequence contains the following first 12 values $[49, 36, 42, 3, 39, 12, 40, 4, 21, 9, 35, 29]$ (Figure 3d).

3. Results

3.1. Dataset B1

Architecture LogNet 51:50:20:2 were considered for B1 dataset. The result of reservoir optimization by the method from section 2.3 with the number of epochs $Ep = 50$ led to the parameters of the congruential generator indicated in Table 5.

Table 5. Optimal reservoir parameters.

Dataset B1				Dataset B2			
K	D	L	C	K	D	L	C
93	68	9276	73	47	99	8941	56

Feature selection was carried out with the number of epochs $Ep = 100$. Prior to selection, the $dA_{51}(z)$ plot shown in Figure 4a. After future selection the redundant future are of numbers $z = 21, 37, 42, 49, 40$, the $dA_{46}(z)$ plot shown in Figure 4b. It can be seen that the influence of features with numbers $z = 20, 19, 10, 17$ has increased.

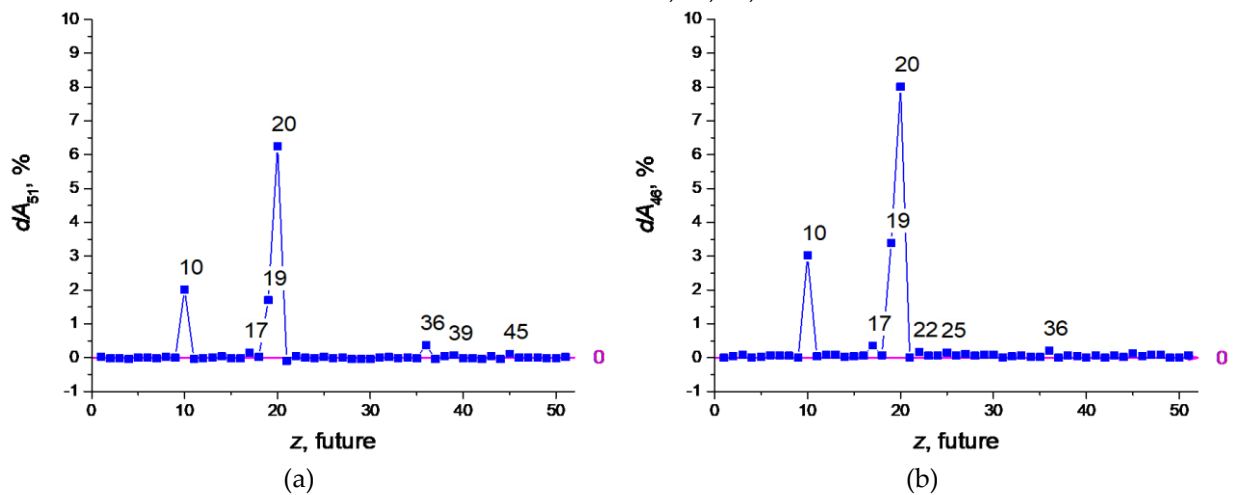


Figure 4. Function of the feature strength $dA_{51}(z)$ (a), $dA_{46}(z)$ (b).

The dependence of $A_{46}(FR[21,37,42,49,40])$ on the number of epochs is shown in Figure 5, the values of other metrics are shown in Table 6.

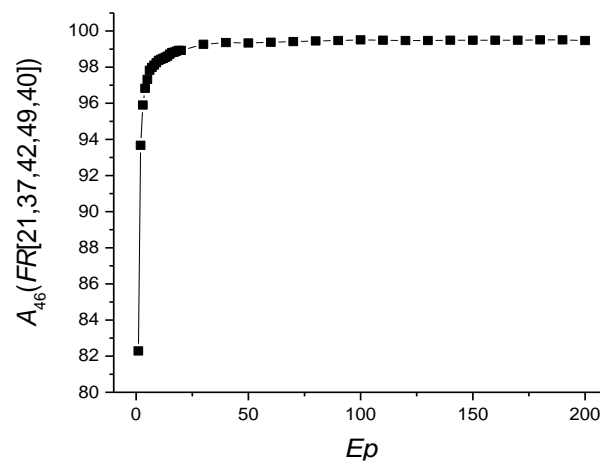


Figure 5. Dependence of $A_{46}(FR[21,37,42,49,40])$ on the number of epochs Ep .

Table 6. Classification metrics depending on the number of training epochs Ep .

Ep	$A_{46}(FR[21,37,42,49,40])$	Precision "non- Covid-19"	Precision "Covid-19"	Recall "non- Covid-19"	Recall "Covid- 19"	F1 "non- Covid-19"	F1 "Covid- 19"
10	98.376	0.978	0.99	0.991	0.977	0.984	0.984
30	99.339	0.992	0.995	0.995	0.992	0.993	0.993
100	99.509	0.994	0.996	0.996	0.994	0.995	0.995
150	99.49	0.994	0.996	0.996	0.994	0.995	0.995
200	99.471	0.994	0.995	0.995	0.994	0.995	0.995

$Ep = 100$ will be taken as the optimal value of the number of epochs. The RBV values found most important in the diagnosis of COVID-19 are the features listed in Table 7. The most important of these are MCHC, MCH and aPTT. MCHC in a blood test allows to find out the average amount of hemoglobin in an erythrocyte.

Table 7. The 7 features found to be most important in the diagnosis of COVID-19.

Number	dA_{46}	Features
20	8.007	MCHC
19	3.399	MCH
10	3.022	aPTT
17	0.359	HCT
36	0.208	HDL-C
22	0.17	MONO
25	0.151	RBC

MCH: mean corpuscular hemoglobin; MCHC: mean corpuscular hemoglobin concentration; aPTT: activated partial prothrombin time; HCT: hematocrit; HDL-C: high-density lipoprotein-cholesterol; MONO: monocyte count; RBC: red blood cells.

Efficiency of LogNNNet in determining the diagnosis of COVID-19 using only 7 features and their combinations shown in Table 8.

Table 8. LogNNNet efficiency for various combinations of features.

Combinations of features	A	Precision "non-Covid- 19"	Precision "Covid-19"	Recall "non- Covid-19"	Recall "Covid- 19"	F1 "non- Covid-19"	F1 "Covid- 19"
$A_{46}(FR[21,37,42,49,40])$	99.509	0.994	0.996	0.996	0.994	0.995	0.995
$A_7(FS[20,19,10,17,36,22,25])$	99.358	0.991	0.996	0.996	0.991	0.994	0.994
$A_1(FS[20])$	94.279	0.930	0.958	0.959	0.926	0.944	0.942
$A_1(FS[19])$	52.418	0.526	0.524	0.500	0.548	0.509	0.532
$A_1(FS[36])$	94.429	0.935	0.955	0.956	0.932	0.945	0.943
$A_2(FS[20,19])$	99.150	0.989	0.994	0.994	0.989	0.992	0.991
$A_2(FS[20,36])$	97.583	0.973	0.979	0.979	0.972	0.976	0.976
$A_2(FS[19,36])$	94.373	0.934	0.955	0.957	0.931	0.945	0.943
$A_3(FS[20,19,10])$	99.169	0.989	0.995	0.995	0.989	0.992	0.992

Thus, even using only one feature 20 (MCHC) or 36 (HDL-C) in determining the diagnosis of COVID-19 provides a high classification accuracy of $A_1(FS[20])$, $A_1(FS[36])$ ~94%. Combination of 2 features 20 (MCHC) and 19 (MCH) allows to reach accuracy $A_2(FS[20,19])$ ~ 99.15%.

When Table 8 is examined, the accuracy rate of the model in diagnosing the disease with 7 features was almost equal to the accuracy rate in using all 46 features (A_7 ~ 99.4 vs. A_{46} ~ 99.59).

3.2. Dataset B2

Architecture LogNNNet 51:50:20:2 were considered for B2 dataset. The result of reservoir optimization by the method from section 2.3 with the number of epochs $Ep = 50$ led to the parameters of the congruential generator indicated in Table 5. Feature selection was carried out at the number of epochs $Ep = 150$. Prior to selection futures strength correspond to $dA_{51}(z)$, see Figure 3a. After feature selection the redundant future are of numbers $z = 44, 45$ and 14 , the $dA_{48}(z)$ graph shown in Figure 3d.

The dependence of $A_{48}(FR[44,45,14])$ on the number of epochs is shown in Figure 6, the values of other metrics are shown in Table 9.

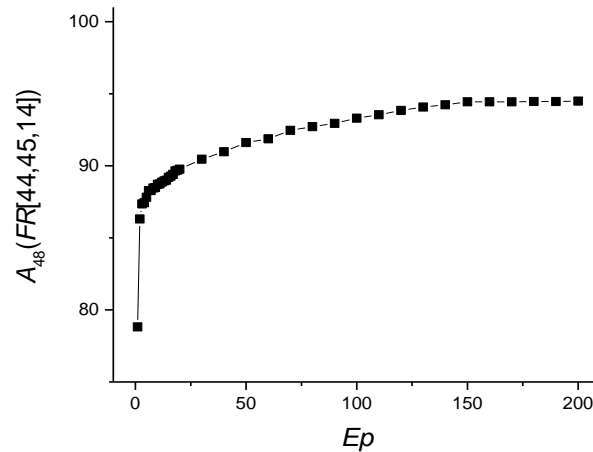


Figure 6. Dependence of $A_{48}(FR[44,45,14])$ on the number of epochs Ep .

Table 9. Classification metrics depending on the number of training epochs Ep .

Ep	$A_{48}(FR[44,45,14])$	Precision "non-ICU"	Precision "ICU"	Recall "non-ICU"	Recall "ICU"	F1 "non-ICU"	F2 "ICU"
10	88.715	0.993	0.307	0.887	0.881	0.937	0.451
30	90.459	0.993	0.347	0.906	0.876	0.947	0.492
100	93.306	0.990	0.433	0.939	0.821	0.964	0.562
150	94.434	0.989	0.49	0.952	0.797	0.97	0.599
200	94.486	0.987	0.495	0.955	0.767	0.97	0.592

$Ep = 150$ will be taken as the optimal value of the number of epochs. The metrics for the "ICU" case are significantly worse than those for the "non-ICU" case, which is also due to the small amount of data for the "ICU" case. The most important routine blood values in identifying severely and mildly infected COVID-19 patients are the features listed in Table 10. The most important of these are ESR and NEU.

Efficiency of LogNNNet when using only the 12 features and their combinations to identify severely and mildly infected COVID-19 patients are shown in Table 11.

Here, the recall value indicates what percentage of individuals diagnosed as mild/severe patients by the specialist could be recognized as mild/severe patients by our model. In other words, the recall value here indicates the success of our model in distinguishing mild or severe patients. Here, the precision value indicates what percentage of the individuals diagnosed as mild/severe patients by our model were also defined as mild/severe patients by the specialist. In other words, the precision value here shows the success of our model in diagnosing mild or severe patients.

Table 10. The 12 features found to be most important in detecting severely (ICU) and mildly (non-ICU) infected COVID-19 patients.

Number	dA_{48}	Features
49	2.18	ESR
36	1.872	NEU
42	1.59	CRP
3	1.359	Albumin
39	1.154	RBC
12	0.974	Chlorine
40	0.872	RDW
4	0.795	ALP
21	0.795	TP
9	0.769	Glucose
35	0.744	MPV
29	0.718	HGB

ESR: erythrocyte sedimentation rate; NEU: neutrophil count; CRP: C-reactive protein; RBC: red blood cells; RDW: red cell distribution width; ALP: alkaline phosphatase; TP: total protein; MPV: mean platelet volume; HGB: hemoglobin.

Table 11. LogNNNet efficiency for various combinations of features.

Combinations of features	A	Precision "non-ICU"	Precision "ICU"	Recall "non- ICU"	Re- call "ICU"	F1 "non- ICU"	F1 "ICU"
$A_{48}(FR[44,45,14])$	94.434	0.989	0.49	0.952	0.797	0.97	0.599
$A_{12}(FS[49,36,42,3,39,12,40,4,21,9,35,29])$	90.946	0.990	0.364	0.914	0.831	0.950	0.499
$A_1(FS[49])$	59.598	0.950	0.059	0.605	0.418	0.694	0.097
$A_1(FS[39])$	75.040	0.955	0.085	0.773	0.341	0.851	0.133
$A_3(FS[49,36,42])$	82.712	0.989	0.210	0.827	0.826	0.900	0.334
$A_7(FS[49,36,42,3,39,12,40])$	89.355	0.991	0.341	0.896	0.846	0.940	0.469

When Table 11 was examined, the accuracy of the model run with 12 features to identify mildly and severely infected patients was close to the accuracy rate of the model run with 48 features ($A_{12} \sim 90.9$ vs $A_{48} \sim 94.94$). In addition, the overall accuracy of our LogNNNet model, which was run with seven features, was 89.3%, its success in diagnosing mildly infected (precision value) 99.1%, and its success in recognizing mildly infected patients (recall value) was 89.6% (Table 11). The metrics for the "ICU" case are significantly worse than those for the "non-ICU" case. Here, it was seen that our model decided in favor of the diagnosis of mildly infected (high precision for non-ICU, low precision for ICU) due to the sample number unbalance of our mildly infected and severely infected patients.

4. Discussion

COVID-19 is a systemic multi-organ damage disease that causes severe acute respiratory syndrome, still causes death and disease in the world and continues to spread [3,46]. Mertoğlu et al. [1] reported that despite the use of vaccine, the spread of the disease could not be stopped and important mutations were detected in the structure of the virus. So it is likely that COVID-19 will continue in our lives. Despite the large number of studies on COVID-19, Kim et al. [47] showed that some of these studies were contradictory and some pathological aspects of the disease could not be fully determined. In previous studies, changes in many RBVs as well as some hematological abnormalities were observed during the course of the disease [6,47]. The fact that most of the patients lost their lives in case of severe infection continued a serious struggle against the disease all over the world

[10,48]. In addition, Brinati et al. [18] and Zhang et al. [48] pointed out that various complications may occur during the treatment process of COVID-19, and this makes it important to predict the prognosis of the disease in the early period. Similarly, Mertoğlu et al. [1] and Huyut and İlkbahar [3] stated that early prediction of the diagnosis/prognosis of the disease is important in the first response to severely infected COVID-19 patients.

As with immunodiagnostic testing, RT-PCR testing may have difficulty identifying true positive and negative individuals infected with COVID-19 [4,49]. Indeed, Teymouri et al. [49] and D'Cruz et al. [50] suggested that to increase the sensitivity of the RT-PCR test, the test should be repeated on multiple samples and the application methodology should be improved. However, these procedures are a troublesome process for health personnel and patients. These difficulties in diagnosing COVID-19 have further increased the importance of RBVs methods [1,2]. In this context, it is possible to determine both the diagnosis and the prognosis of the disease with RBVs (biomarkers), which are easier to obtain, more economical and faster to measure [1–6].

In the ML study for the diagnosis of COVID-19 based on RBVs, Brinati et al. [18] explained that AI models are based on clinical features and could be used for processes such as disease diagnosis and prognosis. Cabitza et al. [19] reported that AI models in which the RBVs are applied can be both an adjunct and an alternative method to rRT-PCR. In addition, Cabitza et al. [19] emphasized that AI application results can provide information about the infection risk level and can be used in rapid triage and quarantine of high-risk patients.

In this study, the most effective RBV biomarkers in the diagnosis and prognosis of COVID-19 were determined by a two-step feature selection procedure for use in peripheral IoT devices with low computing resources. Our LogNNet deep neural network model, fed with selected features, identified sick and healthy individuals, and especially mildly infected patients, with high accuracy and precision.

In the first data set used in this study, the RBVs of COVID-19 positive ($n = 2648$) patients and COVID-19 negative ($n = 2648$) individuals were recorded. In the second data set, the RBVs of 3899 patients ($n = 203$ ICU and $n = 3696$ non-ICU) hospitalized with the diagnosis of COVID-19 were recorded. 51 features of all patients were reached (Table 1 and Table 2). A new two-stage feature selection procedure (see section 2.5) was applied on the datasets and features were found for each dataset. The features selected for the first dataset were fed into LogNNet deep neural network, and the performance of the method in the diagnosis of COVID-19 was obtained. Then, the selected features for the second dataset were fed into LogNNet deep neural network, and the performance of the method in identifying mildly and severely infected patients (determining the prognosis of the disease) was obtained.

In many previous studies on the diagnosis and prognosis of COVID-19, changes in most of the RBV parameters and biomarkers were indicated [1–3,5]. Mertoglu et al. [1] and Yang et al. [51] reported that the most effective RBV biomarkers in the diagnosis/prognosis of COVID-19 are CRP and LYM. However, in other studies conducted for this purpose, blood values of CRP, procalcitonin, ferritin, ALT, aPTT and ESR were reported [3,4,6]. Banerjee et al. [8] used random forest, glmnet, generalized linear models, and ANN neural network models to determine the diagnosis of COVID-19 with 14 RBV values of 81 covid positive and 517 healthy individuals. In that study, glmnet was found to be the most successful model in the diagnosis of the disease with 92% sensitivity and 91% accuracy [8]. Brinati et al. [18] used various ML methods with 13 RBV values for diagnosis of the disease (102 negative 177 covid positive) and noted the models with the highest accuracy were random forest (82%) and logistic regression (78%), respectively. Similarly, Cabitza et al. [19] used various ML models to rapidly detect COVID-19 using many RBV parameters and found the models with the highest accuracy were random forest (88%), support vector machine (SVM) (88%), and k-nearest neighbor (86%), respectively. Joshi et al. [21] developed a trained logistic regression model using some RBVs on a dataset of 380 cases, reporting good sensitivity (93%) but low specificity (43%). Yang et al. [20] applied various

ML models on 27 RBV parameters of a large patient population of 3356 individuals (42% COVID-19 positive), and found the gradient boost tree model to be the most successful model in the diagnosis of the disease with 76%-sensitivity and 80%-specificity value. In a COVID-19 study using chest computed tomography (CT) data and RBV parameters, Mei et al. [22] showed a model combining CNN and multilayer sensor and found the success of the model in diagnosing the disease with 84% sensitivity and 83% specificity. Soares [23], proposed a model combining SVM, ensembling and SMOTE Boost models to diagnose COVID-19 using 15 RBV parameters in a population of 599 individuals, and found the success of the model in diagnosing the disease as 86% specificity and 70% sensitivity. Running various ML models to determine the diagnosis of COVID-19 with the RBV parameters, Soltan et al. [24] found the XGBoost method as the most successful model with 85% sensitivity and 90% precision.

This study found the seven most important biomarkers in the diagnosis of COVID-19 (Table 7). Among these, the most important were MCHC, MCH and aPTT biomarkers. The overall accuracy rate of our LogNNNet model, which was run with seven features found to be important in the diagnosis of the disease, was found to be $A_7(FS[20,19,10,17,36,22, 25]) \sim 99.3\%$, and the rate of precision identification of patients was 99.6%. In addition, when different combinations of features that are important in the diagnosis of patients are examined, the overall accuracy of our LogNNNet model, which was run only with MCHC and MCH features, was $A_2(FS[20,19]) \sim 99.1\%$ and the rate of precision identification of patients 99.4%. In addition, the overall accuracy rate of our model using only the MCHC feature was 94.2%, while the overall accuracy rate of our model using only the HDL-C feature was 94.4%. These results show that our LogNNNet deep neural network model can accurately and precisely detect almost all COVID-19 patients with very few features. In addition, it was understood that the features determined by the feature selection procedure used in this study (Table 7) could be used safely as an alternative diagnostic tool in the diagnosis of the disease.

In many studies, it has been stated that the ALT, AST, LDH, direct bilirubin, and creatine kinase RBVs increase in severe COVID-19 patients, and the hemoglobin values decrease significantly compared to mildly infected patients [6,22,52]. However, in some studies, the LYM, NEU, WBC, MCV, MPV, and RDW hematological RBVs were found to be higher in severe COVID-19 patients when compared to mildly infected patients [1–3,6]. Mousavi et al. [15], Zhang et al. [52], and Zheng et al.[53] determined that patients with severe COVID-19 had lower the EOS, MONO, RBC, hematocrit, hemoglobin and MCV hematological values when compared to mild patients. Huyut et al. [6], showed that the ESR, INR, PT, CRP, D-dimer, and ferritin biomarkers are the most important biomarkers in the mortality of the disease in their study to determine the RBVs that most affected those who died from COVID-19. Luo et al. [54], proposed a Multi-Criteria Decision Making (MCDM) algorithm combining Ideal Solution Similarity Sequencing Technique (TOPSIS) and Naive Bayes (NB) as a feature selection procedure to predict severity of COVID-19 from initial RBV values. With the MCDM model, Luo et al. [54] found that the WBC, LYM, NEU values, and age were the most effective features in determining the severity of the disease, and obtained 82% accuracy by ROC analysis. Similarly, Ma et al.[55] and Lai et al. [56] noted that high the WBC and NEU values are important manifestations of bacterial infection and indicate a serious disease state that complicates the clinical situation.

Similarly, in this study, twelve most important biomarkers were found in determining the prognosis of COVID-19 (identifying severely and mildly infected patients) (Table 10). Among them, the most important ones were ESR, NEU, CRP, albumin and RBC biomarkers, respectively. The overall accuracy of our LogNNNet model, which was run with twelve features, was 90.9%, the success rate in diagnosing mildly infected patients (precision rate) was 99.0%, and the success rate in diagnosing severely infected patients (precision rate) was 36.6% (Table 11). However, the success of our LogNNNet model, which was

run with twelve features, in distinguishing mild or severe patients according to their real conditions (recall value), was 91.4% and 83.1%, respectively (Table 11).

Here, it was seen that our model decided in favor of the diagnosis of mildly infected (high precision for non-ICU, low precision for ICU) due to the sample size instability of our mildly infected and severely infected patients. However, our model showed a high recall value in recognizing/identifying mildly and severely infected patients. For example, it can be said that our model, which was run with only three features, showed an average of 82.6% agreement with the expert opinion in distinguishing (identifying) mildly or severely infected patients (Table 11). However, severe patient diagnosis of our model showed low agreement with expert opinion (low precision “ICU”) (Table 11). Accordingly, the success of our model in diagnosing severe patients is low. As a result, our LogNet model, which is run with the features in Table 11, can be used safely with high sensitivity (recall) to confirm the expert opinion in recognizing mild and severely infected patients. In addition, our model can be an excellent alternative motivation tool for diagnosing mildly infected using the features in Table 11. Furthermore, the success of the LogNet model using very few features in distinguishing mild and severe patients and diagnosing mildly infected patients is remarkable.

Many other studies [18,57,58], confirming the association of the features found in this study with COVID-19 confirm the clinical importance of our model. In addition, the poor performance of our model in diagnosing severe patients (low precision for the ICU) is an expected situation. As a matter of fact, in many studies, it was stated that severe COVID-19 patients experienced more changes in the RBV values than mildly infected patients, and that various complications could occur during the severe disease process [1–3,6]. For this reason, it has been reported that there are many factors affecting the intensive care need of an individual with COVID-19 and difficulties in determining this process with only RBV values [1–6]. Therefore, we know that there are few studies on determining the severity of infection in patients with COVID-19 based on the RBV values alone.

Cabitz et al. [19], Soltan et al. [24], and Rabanser et al. [59] stated that the reported performance values are good enough, especially in terms of screening, considering the economical and rapid results of the developed artificial intelligence models. Moreover, Brinati et al. [18] suggested the necessity of conducting studies on the predictability of arterial blood gas tests in addition to routine blood values for the diagnosis of COVID-19. In this context, we planned our next works as follows. Our initial plan is to identify the diagnosis and prognosis of COVID-19 with LogNet model using the arterial blood gases. Another plan is to determine the mortality of COVID-19 with LogNet model using the RBV values.

Velichko [42] reported the method for estimation the occupied RAM in the implementation of the LogNet on Arduino microcontrollers. The LogNet 51:50:20:2 model, discussed above, takes about 13.7 kB of RAM. As the matrix W occupies ~10.4 kB, if algorithm with RAM saving is used, this memory can be freed, and the algorithm will use ~3.3 kB. Therefore, the model can be placed on microcontrollers with a RAM size of 16 kB, for example, Arduino Nano.

With recent advances in information and communication technologies through the adoption of IoT technology, smart health monitoring and support systems have a higher development and acceptability margin for improved wellness [60,61]. The integration of medical technologies into IoT is called the Internet of Medical Things (IoMT) [62].

In this context, the availability of low-cost single-chip microcontrollers and advances in wireless communication technology have encouraged researchers to design low-cost embedded systems for healthcare monitoring applications [60]. Taiwo and Ezugwu [61] noted that doctors can use patients' data to remotely monitor their physiological health status and diagnose their disorders. In a study designed for mobile health applications, Hu et al. [63] used various graphical biosensors to monitor conditions such as heart attack, brain problems, high blood pressure (seizures, mental disorder, etc.). In a study for a similar purpose, Vizbaras et al. [64] reported that the stretching and bending

vibrations of various chemical bonds are molecule-specific, thus certain infrared spectral ranges are of particular interest in biomedical sensing. In addition, Vizbaras et al.[64] stated that this approach can be used to selectively detect important biomolecules such as glucose, lactate, urea, ammonia, serum albumin, and so on. Clifton et al. [65] demonstrated the use of wearable sensors for the routine healthcare in their study of the large-scale clinical adoption of the "intelligent" predictive monitoring systems..

In this context, mobile sensors for the measurement of routine blood parameters to be used in the real-time detection of various diseases are being developed rapidly with the development of technology [66–69]. Pfeil et al. [66] showed that the RBV values can be measured using a low-cost mobile microscope, an ocular camera, and a smartphone. Chan et al. [67] determined PT and INR blood values by monitoring the micro-mechanical movements of a copper particle with a proof-of-concept using the vibration motor and camera in smartphones. Farooqi et al. [68] followed the diabetic patients with telemonitoring and bluetooth-enabled self-monitoring devices for a while and produced new solutions for the glycemic control of the patients. Zhang et al.[69] determined various biochemical parameters by electrochemical controls.

In this sense, it is anticipated that in the future, the data can be obtained in real time and used to provide immediate medical advice before the health problems of the patients occur/progress. The technique presented in this article can be used to create mobile health monitoring systems.

As a result, the outputs of LogNNet model can be used in different scenarios. Presented feature selection method can be used in conjunction with molecular testing to obtain high sensitivity and certainty regarding suspected cases. Thus, more positive patients can be identified, isolated and treated in a timely manner. Likewise, the outputs of our model can be used while the results of other tests are awaited. The results of this study showed that LogNNet deep neural network models can be used with high performance for clinical decision support systems and mobile diagnostics.

5. Conclusions

Determining mild or severe infection status according to various diagnostic tests and imaging results of COVID-19 patients can be costly, take a long time, and different complications may occur in this process. In this case, the patient's health may be at higher risk and health services may face tragic situations under intense pressure. This study can be a fast, reliable and economical alternative mobile tool for the diagnosis and prognosis of COVID-19 based on the RBV values measured only at the time of admission to the hospital.

In this study, the most effective RBVs in the diagnosis/prognosis of COVID-19 were determined using a new feature selection method for the LogNNet reservoir neural network. The most important RBVs in the diagnosis of the disease were MCHC, MCH and aPTT. The most important RBVs in the prognosis of the disease were ESR, NEU, CRP, albumin and RBC. In this study, the LogNNet deep neural network model accurately and precisely detected almost all COVID-19 patients with very few features. Accordingly, LogNNet was found to be an excellent diagnostic tool with high accuracy and precision in COVID-19. LogNNet-model achieved an accuracy rate of $A_{46} = 99.5\%$ in the diagnosis of the disease with 46 features and $A_3 = 99.17\%$ with only MCHC, MCH, and aPTT features. Model reached an accuracy rate of $A_{48} = 94.4\%$ in determining the prognosis of the disease with 48 features and $A_3 = 82.7\%$ with only ESR, NEU, and CRP features.

In addition, the features determined by the feature selection procedure used in this study can be used accurately and safely to confirm the expert's opinion in recognizing mildly and severely infected patients (high recall value). The LogNNet model, which is trained with the most important features in the prognosis of the disease, can be an excellent alternative motivation tool in the diagnosis of patients with mildly infected covid. Accordingly, our feature selection procedure for LogNNet in this study was found to be

very successful in identifying the most important RBVs in the diagnosis and prognosis of COVID-19.

The LogNNNet model, suitable for peripheral IoT devices with low computing resources, helps optimize the allocation of medical resources. The LogNNNet model demonstrated excellent classification capability for clinical decision support systems running on powerful microcontrollers with small memory size. In addition, it was observed that the LogNNNet model was able to present the risk factors for the presence and prognosis of any disease based on a set of medical health indicators. The results of this study can be safely used in medical peripheral devices of the IoT(IoTM) with low RAM resources, including clinical decision support systems, remote internet medicine and telemedicine.

Supplementary Materials: The following supporting information can be downloaded at: www.mdpi.com/xxx/s1, Dataset_B1_B2.zip, Readme.pdf. Kindly cite our paper when you wish to use this dataset.

Author Contributions: Conceptualization, M.T.H., and A.V.; methodology, M.T.H., and A.V.; software, A.V.; validation, M.T.H., and A.V.; formal analysis, M.T.H.; investigation, A.V.; resources, M.T.H.; data curation, M.T.H.; writing—original draft preparation, M.T.H., and A.V.; writing—review and editing, M.T.H., and A.V.; visualization, M.T.H., and A.V.; supervision, M.T.H.; project administration, M.T.H.; funding acquisition, A.V. All authors have read and agreed to the published version of the manuscript.

Funding: This research was supported by the Russian Science Foundation (grant no. 22-11-00055, <https://rscf.ru/en/project/22-11-00055/>).

Institutional Review Board Statement: The data set used in this study was collected in order to be used in various studies in the estimation of the diagnosis, prognosis and mortality of COVID-19. The necessary permissions for the collected data set were given by the Ministry of Health of the Republic of Turkey and the Ethics Committee of Erzincan Binali Yıldırım University. This study was conducted in accordance with the 1989 Declaration of Helsinki.

Informed Consent Statement: In this study, a data set including only routine blood values, RT-PCR results (positive or negative) and treatment units of the patients was downloaded retrospectively from the information system of our hospital in digital environment. A new sample was not taken from the patients. There is no information in the data set that includes identifying characteristics of individuals. It was stated that routine blood values would only be used in academic studies, and written consent was obtained from the institutions for this. In addition, therefore, written informed consent was not administered for every patient.

Data Availability Statement: The data used in this study can be shared with the parties, provided that the article is cited.

Acknowledgments: We thank the method of Erzincan Mengücek Gazi Training and Research Hospital for their support in reaching the material used in this study. Special thanks to the editors of the journal and to the anonymous reviewers for their constructive criticism and improvement suggestions.

Conflicts of Interest: The authors declare no conflict of interest.

References

1. Mertoglu, C.; Huyut, M.; Olmez, H.; Tosun, M.; Kantarci, M.; Coban, T. COVID-19 is more dangerous for older people and its severity is increasing: a case-control study. *Med. Gas Res.* **2022**, *12*, 51–54, doi:10.4103/2045-9912.325992.
2. Mertoglu, C.; Huyut, M.T.; Arslan, Y.; Ceylan, Y.; Coban, T.A. How do routine laboratory tests change in coronavirus disease 2019? *Scand. J. Clin. Lab. Invest.* **2021**, *81*, 24–33, doi:10.1080/00365513.2020.1855470.
3. Huyut, M.T.; İlkbahar, F. The effectiveness of blood routine parameters and some biomarkers as a potential diagnostic tool in the diagnosis and prognosis of Covid-19 disease. *Int. Immunopharmacol.* **2021**, *98*, doi:10.1016/j.intimp.2021.107838.
4. HUYUT, M.T.; HUYUT, Z. Forecasting of Oxidant/Antioxidant levels of COVID-19 patients by using Expert models with biomarkers used in the Diagnosis/Prognosis of COVID-19. *Int. Immunopharmacol.* **2021**, *100*, doi:10.1016/j.intimp.2021.108127.

5. Huyut, M.; Üstündağ, H. Prediction of diagnosis and prognosis of COVID-19 disease by blood gas parameters using decision trees machine learning model: a retrospective observational study. *Med. Gas Res.* **2022**, *12*, 60–66, doi:10.4103/2045-9912.326002.
6. Tahir Huyut, M.; Huyut, Z.; İlkbahar, F.; Mertoğlu, C. What is the impact and efficacy of routine immunological, biochemical and hematological biomarkers as predictors of COVID-19 mortality? *Int. Immunopharmacol.* **2022**, *105*, doi:10.1016/j.intimp.2022.108542.
7. Guan, W.; Ni, Z.; Hu, Y.; Liang, W.; Ou, C.; He, J.; Liu, L.; Shan, H.; Lei, C.; Hui, D.S.C.; et al. Clinical Characteristics of Coronavirus Disease 2019 in China. *N. Engl. J. Med.* **2020**, *382*, 1708–1720, doi:10.1056/NEJMOA2002032.
8. Banerjee, A.; Ray, S.; Vorselaars, B.; Kitson, J.; Mamalakis, M.; Weeks, S.; Baker, M.; Mackenzie, L.S. Use of Machine Learning and Artificial Intelligence to predict SARS-CoV-2 infection from Full Blood Counts in a population. *Int. Immunopharmacol.* **2020**, *86*, doi:10.1016/j.intimp.2020.106705.
9. Huyut, M.T.; Soygüder, S. The Multi-Relationship Structure between Some Symptoms and Features Seen during the New Coronavirus 19 Infection and the Levels of Anxiety and Depression post-Covid. *East. J. Med.* **2022**, *27*, doi:10.5505/ejm.2022.35336.
10. Amgalan, A.; Othman, M. Hemostatic laboratory derangements in COVID-19 with a focus on platelet count. *Platelets* **2020**, *31*, 740–745, doi:10.1080/09537104.2020.1768523.
11. Li, X.; Wang, L.; Yan, S.; Yang, F.; Xiang, L.; Zhu, J.; Shen, B.; Gong, Z. Clinical characteristics of 25 death cases with COVID-19: A retrospective review of medical records in a single medical center, Wuhan, China. *Int. J. Infect. Dis.* **2020**, *94*, 128–132, doi:10.1016/j.ijid.2020.03.053.
12. Jiang, S.Q.; Huang, Q.F.; Xie, W.M.; Lv, C.; Quan, X.Q. The association between severe COVID-19 and low platelet count: evidence from 31 observational studies involving 7613 participants. *Br. J. Haematol.* **2020**, *190*, e29–e33, doi:10.1111/bjh.16817.
13. Zheng, Y.; Zhang, Y.; Chi, H.; Chen, S.; Peng, M.; Luo, L.; Chen, L.; Li, J.; Shen, B.; Wang, D. The hemocyte counts as a potential biomarker for predicting disease progression in COVID-19: A retrospective study. *Clin. Chem. Lab. Med.* **2020**, *58*, 1106–1115, doi:10.1515/cclm-2020-0377.
14. Lippi, G.; Plebani, M.; Henry, B.M. Thrombocytopenia is associated with severe coronavirus disease 2019 (COVID-19) infections: A meta-analysis. *Clin. Chim. Acta* **2020**, *506*, 145–148, doi:10.1016/j.cca.2020.03.022.
15. Mousavi, S.A.; Rad, S.; Rostami, T.; Rostami, M.; Mousavi, S.A.; Mirhoseini, S.A.; Kiumarsi, A. Hematologic predictors of mortality in hospitalized patients with COVID-19: a comparative study. *Hematol. (United Kingdom)* **2020**, *25*, 383–388, doi:10.1080/16078454.2020.1833435.
16. Beck, B.R.; Shin, B.; Choi, Y.; Park, S.; Kang, K. Predicting commercially available antiviral drugs that may act on the novel coronavirus (SARS-CoV-2) through a drug-target interaction deep learning model. *Comput. Struct. Biotechnol. J.* **2020**, *18*, 784–790, doi:10.1016/j.csbj.2020.03.025.
17. Xu, X.; Jiang, X.; Ma, C.; Du, P.; Li, X.; Lv, S.; Yu, L.; Ni, Q.; Chen, Y.; Su, J.; et al. A Deep Learning System to Screen Novel Coronavirus Disease 2019 Pneumonia. *Engineering* **2020**, *6*, 1122–1129, doi:10.1016/j.eng.2020.04.010.
18. Brinati, D.; Campagner, A.; Ferrari, D.; Locatelli, M.; Banfi, G.; Cabitza, F. Detection of COVID-19 Infection from Routine Blood Exams with Machine Learning: A Feasibility Study. *J. Med. Syst.* **2020**, *44*, doi:10.1007/s10916-020-01597-4.
19. Cabitza, F.; Campagner, A.; Ferrari, D.; Di Resta, C.; Ceriotti, D.; Sabetta, E.; Colombini, A.; De Vecchi, E.; Banfi, G.; Locatelli, M.; et al. Development, evaluation, and validation of machine learning models for COVID-19 detection based on routine blood tests. *Clin. Chem. Lab. Med.* **2021**, *59*, 421–431, doi:10.1515/cclm-2020-1294.
20. Yang, H.S.; Hou, Y.; Vasovic, L. V.; Steel, P.A.D.; Chadburn, A.; Racine-Brzostek, S.E.; Velu, P.; Cushing, M.M.; Loda, M.; Kaushal, R.; et al. Routine Laboratory Blood Tests Predict SARS-CoV-2 Infection Using Machine Learning., doi:10.1093/clinchem/hvaa200.

21. Joshi, R.P.; Pejaver, V.; Hammarlund, N.E.; Sung, H.; Kyu, S.; Lee, H.; Scott, G.; Gombar, S.; Shah, N.; Shen, S.; et al. Short communication A predictive tool for identification of SARS-CoV-2 PCR-negative emergency department patients using routine test results. *J. Clin. Virol.* **2020**, *129*, 104502, doi:10.1016/j.jcv.2020.104502.
22. Mei, X.; Lee, H.C.; Diao, K. yue; Huang, M.; Lin, B.; Liu, C.; Xie, Z.; Ma, Y.; Robson, P.M.; Chung, M.; et al. Artificial intelligence-enabled rapid diagnosis of patients with COVID-19. *Nat. Med.* **2020**, *26*, 1224–1228, doi:10.1038/s41591-020-0931-3.
23. Soares, F. A novel specific artificial intelligence-based method to identify COVID-19 cases using simple blood exams. *medRxiv* **2020**, 2020.04.10.20061036.
24. Soltan, A.A.; Kouchaki, S.; Zhu, T.; Kiyasseh, D.; Taylor, T.; Hussain, Z.B.; Peto, T.; Brent, A.J.; Eyre, D.W.; Clifton, D. Artificial intelligence driven assessment of routinely collected healthcare data is an effective screening test for COVID-19 in patients presenting to hospital. *medRxiv* **2020**, 2020.07.07.20148361.
25. Remeseiro, B.; Bolon-Canedo, V. A review of feature selection methods in medical applications. *Comput. Biol. Med.* **2019**, *112*, 103375, doi:https://doi.org/10.1016/j.compbiomed.2019.103375.
26. Bikku, T. Multi-layered deep learning perceptron approach for health risk prediction. *J. Big Data* **2020**, *7*, doi:10.1186/s40537-020-00316-7.
27. Battineni, G.; Chintalapudi, N.; Amenta, F. Machine learning in medicine: Performance calculation of dementia prediction by support vector machines (SVM). *Informatics Med. Unlocked* **2019**, *16*, 100200, doi:https://doi.org/10.1016/j.imu.2019.100200.
28. Xing, W.; Bei, Y. Medical Health Big Data Classification Based on KNN Classification Algorithm. *IEEE Access* **2020**, *8*, 28808–28819, doi:10.1109/ACCESS.2019.2955754.
29. Hoodbhoy, Z.; Noman, M.; Shafique, A.; Nasim, A.; Chowdhury, D.; Hasan, B. Use of machine learning algorithms for prediction of fetal risk using cardiocographic data. *Int. J. Appl. Basic Med. Res.* **2019**, *9*, 226, doi:10.4103/ijabmr.ijabmr_370_18.
30. Alam, M.Z.; Rahman, M.S.; Rahman, M.S. A Random Forest based predictor for medical data classification using feature ranking. *Informatics Med. Unlocked* **2019**, *15*, 100180, doi:https://doi.org/10.1016/j.imu.2019.100180.
31. Schober, P.; Vetter, T.R. Logistic Regression in Medical Research. *Anesth. Analg.* **2021**, *132*, 365–366, doi:10.1213/ANE.0000000000005247.
32. Podgorelec, V.; Kokol, P.; Stiglic, B.; Rozman, I. Decision trees: An overview and their use in medicine. *J. Med. Syst.* **2002**, *26*, 445–463.
33. Guyon, I.; Gunn, S.; Nikravesh, M.; Zadeh, L.A. *Feature Extraction: Foundations and Applications*; Studies in Fuzziness and Soft Computing; Springer Berlin Heidelberg, 2008; ISBN 9783540354888.
34. Hall, M.A. Correlation-based Feature Selection for Machine Learning. **1999**.
35. Dash, M.; Liu, H. Consistency-based search in feature selection. *Artif. Intell.* **2003**, *151*, 155–176, doi:10.1016/S0004-3702(03)00079-1.
36. Zhao, Z.; Liu, H. Searching for interacting features. *IJCAI Int. Jt. Conf. Artif. Intell.* **2007**, 1156–1161.
37. Hall, M.A.; Smith, L.A. Practical feature subset selection for machine learning 1998, *Volume 20*, 181–191.
38. Kononenko, I. Estimating attributes: Analysis and extensions of RELIEF. *Lect. Notes Comput. Sci. (including Subser. Lect. Notes Artif. Intell. Lect. Notes Bioinformatics)* **1994**, *784 LNCS*, 171–182, doi:10.1007/3-540-57868-4_57.
39. Le Thi, H.A.; Nguyen, V.V.; Ouchani, S. Gene selection for cancer classification using DCA. *Lect. Notes Comput. Sci. (including Subser. Lect. Notes Artif. Intell. Lect. Notes Bioinformatics)* **2008**, *5139 LNAI*, 62–72, doi:10.1007/978-3-540-88192-6_8.
40. Shrinkage, R. Regression Shrinkage and Selection via the Lasso Author (s): Robert Tibshirani Source : Journal of the Royal Statistical Society . Series B (Methodological), Vol . 58 , No . 1 (1996), Published by : Wiley for the Royal Statistical Society Stable URL. **2016**, *58*, 267–288.
41. Velichko, A. Neural network for low-memory IoT devices and MNIST image recognition using kernels based on logistic map.

- Electron.* **2020**, *9*, 1–16, doi:10.3390/electronics9091432.
42. Velichko, A. A method for medical data analysis using the lognet for clinical decision support systems and edge computing in healthcare. *Sensors* **2021**, *21*, doi:10.3390/s21186209.
43. Velichko, A.; Heidari, H. A Method for Estimating the Entropy of Time Series Using Artificial Neural Networks. *Entropy* **2021**, *23*, doi:10.3390/e23111432.
44. Izotov, Y.A.; Velichko, A.A.; Boriskov, P.P. Method for fast classification of MNIST digits on Arduino UNO board using LogNNNet and linear congruential generator. *J. Phys. Conf. Ser.* **2021**, *2094*, 32055, doi:10.1088/1742-6596/2094/3/032055.
45. Heidari, H.; Velichko, A. An improved LogNNNet classifier for IoT application. **2021**.
46. Mattiuzzi, C.; Lippi, G. Which lessons shall we learn from the 2019 novel coronavirus outbreak? *Ann. Transl. Med.* **2020**, *8*, 48–48, doi:10.21037/atm.2020.02.06.
47. Kim, S.; Kim, D.-M.; Lee, B. Insufficient Sensitivity of RNA Dependent RNA Polymerase Gene of SARS-CoV-2 Viral Genome as Confirmatory Test using Korean COVID-19 Cases. *Preprints* **2020**, 1–4, doi:10.20944/preprints202002.0424.v1.
48. Zhang, J. jin; Cao, Y. yuan; Tan, G.; Dong, X.; Wang, B. chen; Lin, J.; Yan, Y. qin; Liu, G. hui; Akdis, M.; Akdis, C.A.; et al. Clinical, radiological, and laboratory characteristics and risk factors for severity and mortality of 289 hospitalized COVID-19 patients. *Allergy Eur. J. Allergy Clin. Immunol.* **2021**, *76*, 533–550, doi:10.1111/all.14496.
49. Teymouri, M.; Mollazadeh, S.; Mortazavi, H.; Naderi Ghale-noie, Z.; Keyvani, V.; Aghababaei, F.; Hamblin, M.R.; Abbaszadeh-Goudarzi, G.; Pourghadamyari, H.; Hashemian, S.M.R.; et al. Recent advances and challenges of RT-PCR tests for the diagnosis of COVID-19. *Pathol. Res. Pract.* **2021**, *221*, 153443, doi:10.1016/j.prp.2021.153443.
50. D’Cruz, R.J.; Currier, A.W.; Sampson, V.B. Laboratory Testing Methods for Novel Severe Acute Respiratory Syndrome-Coronavirus-2 (SARS-CoV-2). *Front. Cell Dev. Biol.* **2020**, *8*, 1–11, doi:10.3389/fcell.2020.00468.
51. Yang, A.P.; Liu, J. ping; Tao, W. qiang; Li, H. ming The diagnostic and predictive role of NLR, d-NLR and PLR in COVID-19 patients. *Int. Immunopharmacol.* **2020**, *84*, 106504, doi:10.1016/j.intimp.2020.106504.
52. Zhang, C.; Shi, L.; Wang, F.S. Liver injury in COVID-19: management and challenges. *Lancet Gastroenterol. Hepatol.* **2020**, *5*, 428–430, doi:10.1016/S2468-1253(20)30057-1.
53. Zheng, M.; Gao, Y.; Wang, G.; Song, G.; Liu, S.; Sun, D.; Xu, Y.; Tian, Z. Functional exhaustion of antiviral lymphocytes in COVID-19 patients. *Cell. Mol. Immunol.* **2020**, *17*, 533–535, doi:10.1038/s41423-020-0402-2.
54. Luo, J.; Zhou, L.; Feng, Y.; Li, B.; Guo, S. The selection of indicators from initial blood routine test results to improve the accuracy of early prediction of COVID-19 severity. *PLoS One* **2021**, *16*, 1–18, doi:10.1371/journal.pone.0253329.
55. Ma, Y.; Hou, L.; Yang, X.; Huang, Z.; Yang, X.; Zhao, N.; He, M.; Shi, Y.; Kang, Y.; Yue, J.; et al. The association between frailty and severe disease among COVID-19 patients aged over 60 years in China: a prospective cohort study., doi:10.1186/s12916-020-01761-0.
56. Lai, C.C.; Shih, T.P.; Ko, W.C.; Tang, H.J.; Hsueh, P.R. Severe acute respiratory syndrome coronavirus 2 (SARS-CoV-2) and coronavirus disease-2019 (COVID-19): The epidemic and the challenges. *Int. J. Antimicrob. Agents* **2020**, *55*, 105924, doi:10.1016/j.ijantimicag.2020.105924.
57. Pan, F.; Ye, T.; Sun, P.; Gui, S.; Liang, B.; Li, L.; Zheng, D.; Wang, J.; Hesketh, R.L.; Yang, L.; et al. Time Course of Lung Changes On Chest CT During Recovery From 2019 Novel Coronavirus (COVID-19) Pneumonia. *Radiology* **2020**, 200370, doi:10.1148/radiol.2020200370.
58. Dahai Zhao; Feifei Yao; Lijie Wang; Ling Zheng; Yongjun Gao; Jun Ye; Feng Guo; Hui Zhao; Rongbao Gao A Comparative Study on the Clinical Features of Coronavirus 2019 (COVID-19) Pneumonia With Other Pneumonias. *Clin. Infect. Dis.* **2020**, *71*, 756–761.
59. Rabanser, S.; Günemann, S.; Lipton, Z.C. Failing loudly: An empirical study of methods for detecting dataset shift. *Adv. Neural Inf. Process. Syst.* **2019**, *32*.

-
60. Al-Aubidy, K.M.; Derbas, A.M.; Al-Mutairi, A.W. Real-time patient health monitoring and alarming using wireless-sensor-network. *13th Int. Multi-Conference Syst. Signals Devices, SSD 2016* **2016**, 416–423, doi:10.1109/SSD.2016.7473672.
 61. Taiwo, O.; Ezugwu, A.E. Smart healthcare support for remote patient monitoring during covid-19 quarantine. *Informatics Med. Unlocked* **2020**, *20*, 100428, doi:10.1016/j.imu.2020.100428.
 62. Lamonaca, F.; Balestrieri, E.; Tudosa, I.; Picariello, F.; Carnì, D.L.; Scuro, C.; Bonavolontà, F.; Spagnuolo, V.; Grimaldi, G.; Colaprico, A. An Overview on Internet of Medical Things in Blood Pressure Monitoring. In Proceedings of the 2019 IEEE International Symposium on Medical Measurements and Applications (MeMeA); 2019; pp. 1–6.
 63. Hu, F.; Xiao, Y.; Hao, Q. Congestion-aware, loss-resilient bio-monitoring sensor networking for mobile health applications. *IEEE J. Sel. Areas Commun.* **2009**, *27*, 450–465, doi:10.1109/JSAC.2009.090509.
 64. Vizbaras, A.; Simonyte, I.; Droz, S.; Torcheboeuf, N.; Miasojedovas, A.; Trinkunas, A.; Buciuinas, T.; Dambrauskas, Z.; Gulbinas, A.; Boiko, D.L.; et al. GaSb Swept-Wavelength Lasers for Biomedical Sensing Applications. *IEEE J. Sel. Top. Quantum Electron.* **2019**, *25*, 1–12, doi:10.1109/JSTQE.2019.2915967.
 65. Clifton, L.; Clifton, D.A.; Pimentel, M.A.F.; Watkinson, P.J.; Tarassenko, L. Predictive monitoring of mobile patients by combining clinical observations with data from wearable sensors. *IEEE J. Biomed. Heal. Informatics* **2014**, *18*, 722–730, doi:10.1109/JBHI.2013.2293059.
 66. Pfeil, J.; Nechyporenko, A.; Frohme, M.; Hufert, F.T.; Schulze, K. Examination of blood samples using deep learning and mobile microscopy. *BMC Bioinformatics* **2022**, *23*, 1–14, doi:10.1186/s12859-022-04602-4.
 67. Chan, J.; Michaelsen, K.; Estergreen, J.K.; Sabath, D.E.; Gollakota, S. Micro-mechanical blood clot testing using smartphones. *Nat. Commun.* **2022**, *13*, 1–12, doi:10.1038/s41467-022-28499-y.
 68. Farooqi, M.H.; Abdelmannan, D.K.; Mubarak, M.; Abdalla, M.; Hamed, A.; Xavier, M.; Joyce, T.; Cadiz, S.; Nawaz, F.A. The Impact of Telemonitoring on Improving Glycemic and Metabolic Control in Previously Lost-to-Follow-Up Patients with Type 2 Diabetes Mellitus : A Single-Center Interventional Study in the United Arab Emirates. **2022**, 2022.
 69. Zhang, Y.; Zhang, Y.; Li, H.; Cao, Y.; Han, S.; Zhang, K.; He, W. Covalent Biosensing Polymer Chain Reaction Enabling Periphery Blood Testing to Predict Tumor Invasiveness with a Platelet Procarcancerous Protein. *Anal. Chem.* **2022**, *94*, 1983–1989, doi:10.1021/acs.analchem.1c03349.